

# Simplified spinal cord phantom for evaluation of SQUID magnetospinography

Y Adachi<sup>1</sup>, D Oyama<sup>1</sup>, N Somchai<sup>2</sup>, S Kawabata<sup>3</sup>, and G Uehara<sup>1</sup>

<sup>1</sup>Applied Electronics Laboratory, Kanazawa Institute of Technology, Ishikawa, Japan

<sup>2</sup>Osaka University Graduate School, Osaka, Japan

<sup>3</sup>Tokyo Medical and Dental University, Tokyo Japan

E-mail: adachi.y+ieee@gmail.com

**Abstract.** Spinal cord functional imaging by magnetospinography (MSG) is a noninvasive diagnostic method for spinal cord diseases. However, the accuracy and spatial resolution of lesion localization by MSG have barely been evaluated in detail so far. We developed a simplified spinal cord phantom for MSG evaluation. The spinal cord phantom is composed of a cylindrical vessel filled with saline water, which acts as a model of a neck. A set of modeled vertebrae is arranged in the cylindrical vessel, which has a neural current model made from catheter electrodes. The neural current model emulates the current distribution around the activated site along the axon of the spinal cord nerve. Our MSG system was used to observe the magnetic field from the phantom; a quadrupole-like pattern of the magnetic field distribution, which is a typical distribution pattern for spinal cord magnetic fields, was successfully reproduced by the phantom. Hence, the developed spinal cord phantom can be used to evaluate MSG source analysis methods.

## 1. Introduction

Magnetospinography (MSG) is a newly developed noninvasive diagnostic method for the spinal cord diseases; MSG is based on superconducting quantum interference device (SQUID) biomagnetic measurements and magnetic source analysis [1]. Weak magnetic fields produced by the neural activity of a spinal cord are detected by an array of SQUID magnetic flux sensors. The transition of the neural current along the spinal cord is visualized by applying magnetic source analysis to the acquired magnetic field data [2]. This is vital information for the diagnoses of spinal cord diseases because the neural signal propagation along a spinal cord reconstructed by magnetic source analysis shows decreases and delays at spinal cord lesions. This is impossible to do when relying only on traditional anatomical information from X-rays computed tomography (CT), or magnetic resonance imaging (MRI). MSG is the only method that provides the functional information of the spinal cord.

To evaluate the accuracy and spatial resolution of lesion localization by MSG, a well-defined spinal cord phantom is necessary, just as in the cases of magnetoencephalography (MEG) [3] or magnetocardiography (MCG) [4]. Therefore, we are currently developing a spinal cord phantom to evaluate the accuracy and spatial resolution of MSG. The phantom simulates the structure of the conductivity distribution around the spinal cord by means of a plastic vessel filled with saline water and plastic vertebrae models. The distribution of the current produced by the neural activity of the spinal cord is artificially reproduced by electrodes dipped in the saline water. The magnetic field generated by this artificial neural current is recorded by the MSG system, and magnetic source



analysis is applied to the magnetic field distribution data. The accuracy of the MSG measurement system and algorithm of the magnetic source analysis can be evaluated by comparing the location of the magnetic sources estimated from the magnetic field measurement with the actual location of the magnetic sources known in advance.

In this paper, we describe a simplified spinal cord phantom comprising a neural current model using catheter electrodes and vertebral bone model in detail.

## 2. Simplified spinal cord phantom

The source of the magnetic field produced by the spinal cord is the local current distributed in the vicinity of the neural signals propagating along the spinal cord. This local current distribution comprises an intracellular current, which is modeled by using two current dipoles oriented in opposite directions, and an extracellular volume current that compensates for the intracellular current, as shown in figure 1(a). Each vertebral bone has a circular structure and is arranged on a line to make a tubular structure surrounding the spinal cord. The vertebral bones act as insulators, but the extracellular volume current passes through the intervertebral space and is distributed outside the spine. This extracellular volume current out of the spine also contributes to the MSG signals along with the extracellular volume current in the vertebral canal.

The spinal cord phantom has the same topological structure as the spine and its surroundings to emulate the intracellular current and extracellular volume current distributed in both the inner and outer areas of the spine.

### 2.1. Neural current model using catheter electrodes

The neural current model using catheter electrodes, which we previously reported [5], was applied to emulate two oppositely directed current dipoles and the extracellular volume current distribution in the spinal cord phantom. Figure 1(b) shows the structure and dimensions of the catheter electrodes. Two sets of two platinum electrodes with thin platinum wire are embedded in a Teflon tube. Two small current elements are formed when the tube is dipped in saline water and a current is run through the electrodes, as shown in figure 1(b); between electrodes A and B and between electrodes C and D. These current elements were assumed to be the current dipoles for the intracellular current. The magnetic field from the currents flowing in reverse to each other can be negligible because the currents cancel each other out. The volume current in the saline water first and foremost closes the current loop, as shown in figure 1(c).

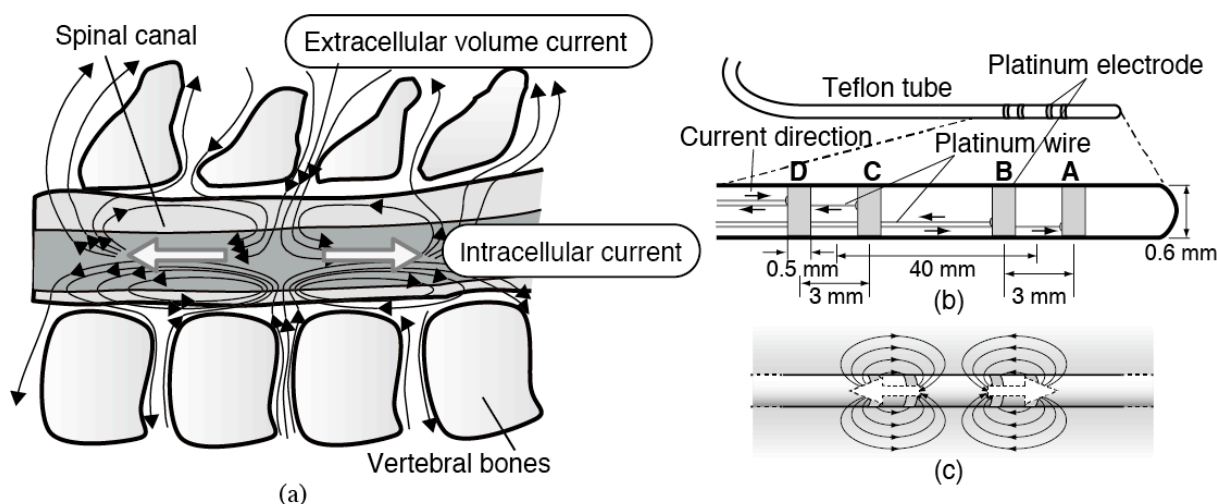


**Figure 1.** (a) Schematic diagram of neural current distribution accompanying spinal cord neural activity; (b) structure and dimensions of catheter electrodes for neural current model; (c) emulated current distribution by neural current model in saline water.

## 2.2. Vertebral bones model

For simplification, an acrylic plastic equilateral triangle prism is used to model a vertebral bone. The thickness and side length of each prism are 12 mm and 22.5 mm, respectively. One of the prism tips represents a spinous process. Each prism has a circular aperture of 20 mm in diameter at the center of the triangle. An array of 18 prisms arranged along a straight line is fixed in a cylindrical vessel positioned horizontally, as shown in figure 2. The gap between adjacent prisms is 1 mm. The center holes of each prism are aligned; this represents the spinal canal. The prism tips representing the spinous processes come close to the lower inner side of the cylindrical vessel to represent the spine of a subject lying in a supine position. There is a slit to embed the prism array on the upper side of the cylindrical vessel. The neural current model described in the previous section is inserted into the holes of the prism array in the cylindrical vessel. The position of the neural current model is shifted 5 mm below the center of the holes. When the cylindrical vessel is filled with saline water, the conductivity distribution along the spinal cord and the surrounding vertebrae bones is simplified but topologically reproduced. This is called a simplified spinal cord phantom.

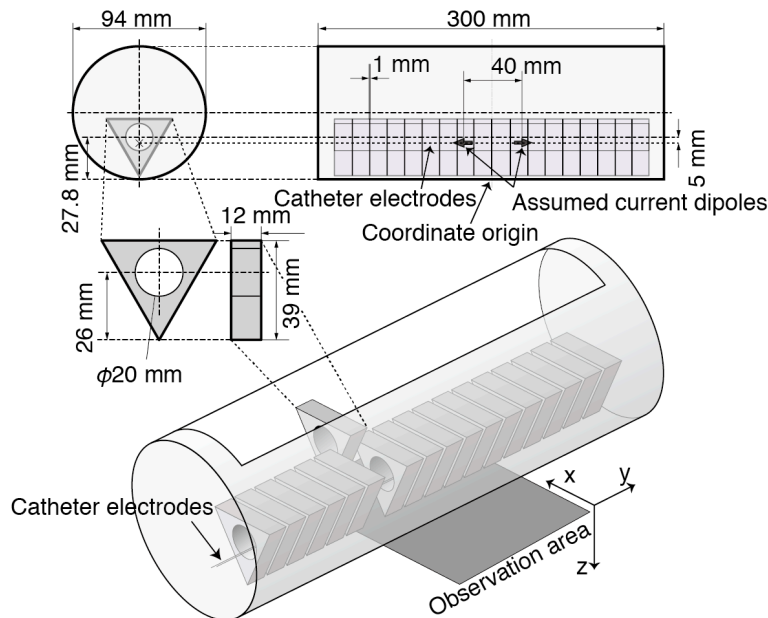


**Figure 2.** Structure and dimensions of spinal cord phantom with vertebral bones model.

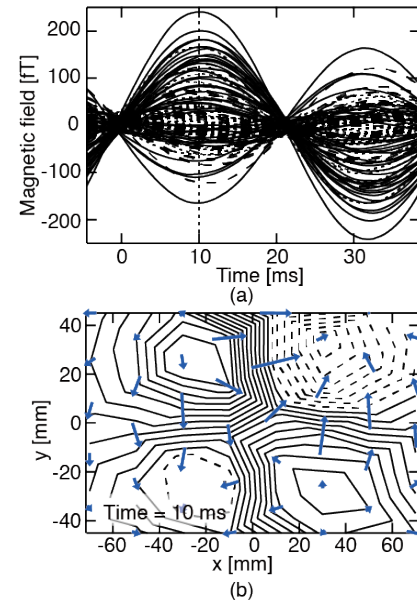


**Figure 3.** (a) Example of magnetic signal waveforms from phantom; (b) magnetic field distribution from phantom.

## 3. Evaluation of magnetic source analysis methods using the simplified spinal cord phantom

### 3.1. Measurement of the emulated spinal cord produced magnetic field

The distribution of the magnetic field produced from the simplified spinal cord phantom was recorded with the previously developed SQUID MSG system [6]. The SQUID MSG system was equipped with an array of 40 vector-type SQUID gradiometers covering the observation area of 90 mm × 140 mm.

The simplified spinal cord phantom was placed on the observation area of the SQUID MSG system. The relative position between the sensor array and phantom was given by localization of the marker coils attached to predetermined sites of the phantom [7]. The two current dipoles of the neural current model were activated by a 23-Hz sinusoidal electric current alternatively chopped at 1 kHz [5]. The signals from each SQUID sensor were filtered by a 100-Hz low-pass filter and digitized at 1 kHz. Figure 3 shows the acquired waveforms and magnetic field distribution at the peak latency. A quadrupole-like pattern was clearly observed along with the typical magnetic field distribution obtained by the actual MSG measurement.

### 3.2. Localization of equivalent current dipoles

To demonstrate the effectiveness of the phantom, equivalent current dipole (ECD) localization was applied to the magnetic field distribution shown in figure 3(b). Three methods were examined to solve the forward problem with searching for the appropriate ECDs; (a) Sarvas' equation, which assumes a horizontally layered conductor model [8]; (b) the boundary element method (BEM), which is based on Geselowitz' equations [9] assuming a cylinder conductor model composed of 20,000 triangle meshes and 10,002 vertices; and (c) the BEM based on Geselowitz' equations assuming a cylinder conductor and prism array insulator model composed of 39,610 triangle meshes and 19,807 vertices.

Table 1 summarizes the ECD localization results; displacement from the assumed ECDs, distance between two of the estimated ECDs, moment of the estimated ECDs, and goodness of fit. The assumed distance and moment were 40 mm and 48 nAm, respectively.

The results of the three methods were compared to each other. In terms of the distance between the two ECDs and their moments, method (c) provided the most reliable ECDs, although the computational cost of the boundary element method was the highest. Thus, the simplified spinal cord phantom was found to be useful for evaluating the performance of the MSG system and magnetic source analysis methods.

**Table 1.** Results of equivalent current dipoles localization.

		(a)	(b)	(c)	Assumed
Displacement	ECD 1	4.7 mm	4.9 mm	4.3 mm	
	ECD 2	3.1 mm	2.5 mm	2.6 mm	
	Average	3.9 mm	3.7 mm	3.5 mm	
Distance between ECDs		38.7 mm	45.0 mm	41.8 mm	40.0 mm
Moment	ECD 1	19.5 nAm	42.6 nAm	49.8 nAm	48.0 nAm
	ECD 2	16.9 nAm	27.9 nAm	32.9 nAm	48.0 nAm
	Average	18.2 nAm	35.3 nAm	41.4 nAm	48.0 nAm
Goodness of fit (GoF)*		83.5%	86.3%	86.6%	—

$$*\text{GoF} = 1 - \frac{\sum(\text{calculated field} - \text{measured field})^2}{\sum(\text{measured field})^2}$$

## 4. Conclusion

We developed a simplified spinal cord phantom to evaluate the accuracy and resolution of the MSG system. The developed phantom was demonstrated to be useful for the evaluation and comparison of several magnetic source analysis methods. We will investigate the origin of the estimation errors for the ECDs in a future study.

## References

- [1] Curio G, Ern  SN, Sandfort J, Sheer J, Stehr R, Trahms L 1991 *Electroenc. Clin. Neurophysiol.* **81** 450–453
- [2] Adachi Y, Oyama D, Kawabata S, Sekihara K, Haruta Y, Uehara G 2013 *IEICE Trans. Electron.* **E96-C**, 326–333
- [3] Yamamoto T, Williamson SJ, Kaufman L, Nicholson C, Llin s R 1988 *Proc. Nat. Aca. Sci. USA* **85** 8732–8736
- [4] Tenner U, Hauelsen J, Nowak H, Leder U, Brauer H 1999 *Phys. Med. Biol.* **44** 1969–1981
- [5] Adachi Y, Oyama D, Kawabata S, Sato M, Uehara G 2011 *IEEE Trans. Mag.* **47** 3837–3840
- [6] Adachi Y, Miyamoto M, Kawai J, Uehara G, Ogata H, Kawabata S, Sekihara K, Kado H 2011 *IEEE Trans. Appl. Supercond.* **21** 485–488
- [7] Ern  SN, Narici L, Pizzella V, Romani GL 1987 *IEEE Trans. Mag.* **MAG-23** 1319–1322
- [8] J. Sarvas 1987 *Phys. Med. Biol.* **32** 11–22
- [9] Geselowitz DB 1970 *IEEE Trans. Mag.* **MAG-6** 346–347

## Acknowledgement

This study was partly supported by the SECOM Science and Technology Foundation.